Finite-element Adaptive Meshing Statistics of Liquid Crystal Coaxial Phase Shifters for mmW Electronics and THz Photonics Beyond Display: A Comparative Study

Jinfeng Li,[*1,2] and Haorong Li[1]

[1]*Beijing Key Laboratory of Millimeter Wave and Terahertz, Beijing Institute of Technology, Beijing, 100081, China,*
[2]*Electrical and Electronic Engineering Department, Imperial College London, London SW7 2AZ, United Kingdom*

Received April 28, 2024; accepted September 29, 2024; published September 30, 2024

Abstract—mmW and THz frequencies offer ultra-high-speed communications for next-generation 5G/6G networks, wherein research advancing the understanding will benefit the electronics and photonics community. Specifically, meshing resolutions across varying frequency ranges and material properties are central to the solution accuracy, reliability, and cost (memory and time) of computational mmW and THz simulations, particularly for the emerging reconfigurable coaxial phase shifters employing nematic liquid crystals (LCs) as tunable media. In the present study, a comparative meshing statistics analysis is conducted for two devices designed for 60 GHz and 0.3 THz, respectively. Each design features two distinct tuning states (LC permittivity of 2.754 and 3.3, respectively), all pertinent to the coaxial TEM (Transverse Electromagnetic) mode. By quantifying the broadband meshing and solution statistics of diverse frequencies and dielectric tuning states for the first time, we establish memory-conserving computational metrology involving reconfigurable coaxial devices operationalized with LC-filled tunable dielectrics tailored for mmW electronics and THz photonics.

Frequency is pivotal in distinguishing disciplines from electrostatics and radio frequency domains including microwave (MW) and millimeter-wave (mmW) to terahertz (THz) and optical wavelengths. The longstanding THz electronics-photonics gap is being bridged with advancements and deepened understanding of device technologies. Frequency also underpins dielectric dispersions and influences the geometry design of dielectric-filled functional devices, e.g., liquid crystal (LC) on silicon (LCOS) devices [1] operating in optical frequencies differing in size and topology significantly against LC tunable mmW phase shifters [2], albeit both are phase-only reconfigurable devices. More specifically, the tunable permittivity of nematic LC stands out as a critical parameter governing the performance limit of LC-based phase reconfigurable electronic components (e.g., our 60 GHz coaxial delay line [2]) and photonic devices (e.g., our 0.3 THz coaxial phase modulator [3]) beyond the conventional display applications of LC.

With the anisotropic-shaped LC molecules being the nano-scale materials and the accommodating geometries largely being in the millimeter scales, the design of LC-combined mmW and THz devices is arguably a multi-physics multi-scale problem, wherein closed-form solution methods are technically infeasible. This motivates the use of numerical solution approaches by discretizing the structure. While our existing studies report the performance results of scattering parameters and constitutive loss comparison between designs for 60 GHz [2] and 0.3 THz [3] by way of illustration, the numerical implications from the discretizing perspective have yet to be clear. To this end, we bridge the gap for both research and education purposes, by embarking on finite-element adaptive meshing studies into the frequency-dependent interactions with variable permittivity states and their computational implications (number of meshed elements, memory required and running time) underpinning the nematic LC and the coaxial designs. As depicted in Fig. 1, coaxially accommodating structures and the tuning states of nematic LC as we proposed [2] and operationalized [3] continue to be deployed as the reliable computing testing ground of LC mmW and THz phase shifters, due to the single-dielectric dominance by a full metal envelope, and hence the noise-free TEM propagation.

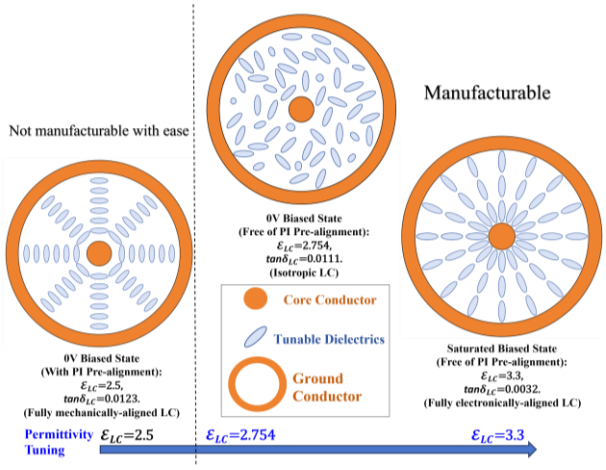

Fig. 1. Cross-section of LC-coaxially-filled variable phase shifter.

As graphically explained in Fig. 1 and examined in our recent works [2,3], the operational (manufacturable) states range from the 0 V bias (isotropic LC state) to the saturated bias state of LC, corresponding to the GT3-24002 LC

* jinfengcambridge@bit.edu.cn

permittivity (ε_{LC}) from 2.754 to 3.3, respectively. As per our permittivity benchmark [2], the effective permittivity of the coaxial transmission line can be approximated as equaling the filled LC's permittivity (ε_{LC}), with an accuracy of between 99.82% and 99.9% for the two extreme tuning states of LC (i.e., ε_{LC} of 2.5 and 3.3, respectively, for the intrinsic dielectric properties of the LC material grade utilized [4]). Notably, the alignment manufacturability limits the operational range of ε_{LC} from 2.754, instead of 2.5, as was explicitly discussed in [2].

Ansys HFSS 3D FEM (finite-element method) solver is used assuming surface roughness-free to start with. The initial mesh is generated by combined TAU (Triangular Adaptive Uniform) [5] and classic methods [6], actioned with wavelength refinements. The workstation employed is based on 11th Gen Intel Core (i5-1155G7) operating at 2.50 GHz. The processor has 4 cores and 8 logical processors, with a random-access memory of 16 GB. The meshing grids are visualized in Fig. 2 for our LC-filled coaxial phase shifters, i.e., 60 GHz design [2] and 0.3 THz design [3], both in the 1 cm (per-unit-length) format and 50 Ω matched at the respective LC tuning states, but differing in the cross-section sizes, due to the diverse vulnerabilities of higher-order mode cutoff that is linked with frequency. The 60 GHz design has an LC thickness (radially) of 0.34876 mm for a core line diameter of 0.23 mm (50 Ω matched on ε_{LC} of 2.8), while the 0.3 THz design is with LC thickness of 0.0895 mm for a core diameter of 0.0505 mm (50 Ω matched on ε_{LC} of 3.3). The nonlinearly dispersive media assumption for LC is not incorporated to purely reflect on the frequency-geometry scaling effect across a broad spectrum (from gigahertz to terahertz).

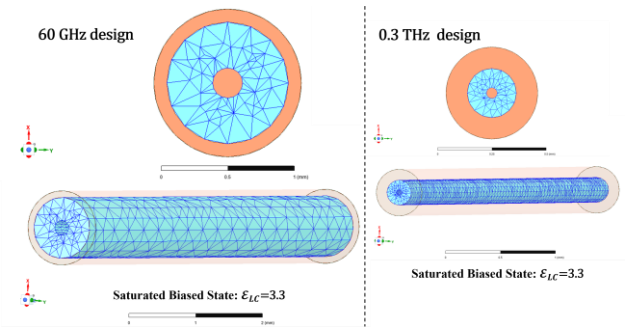

Fig. 2. Broadband unstructured triangulated initial mesh illustrations of LC-coaxially-filled variable phase shifter designs (60 GHz and 300 GHz).

Both designs are targeted the same convergence criterion in S-parameters (maximum delta S of less than 0.01 dB between two consecutive passes) for a fair comparison. Fig. 3 reports the convergence evolution for the two frequency designs (and two dielectric states for each design). The generated meshing elements, encompassing volume meshes (tetrahedral) and surface meshes (triangulated) together, are evolving with the pass number, as quantified in Fig. 4. Albeit dispersion is not considered, the computational resources required for variable permittivity tuning (ε_{LC} of 2.754 vs. 3.3) are quantified and compared in Fig. 5. This is arguably a material mapping problem, with the detailed meshing statistics, run time, and memory usage recorded and presented in Table 1, based on a total number of 8 processes/cores.

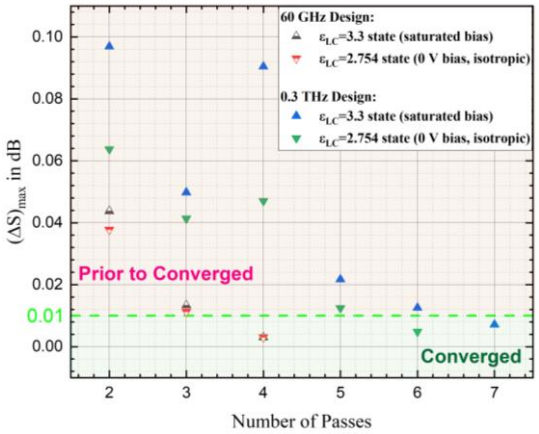

Fig. 3. Convergence evolution of each design and tuning state.

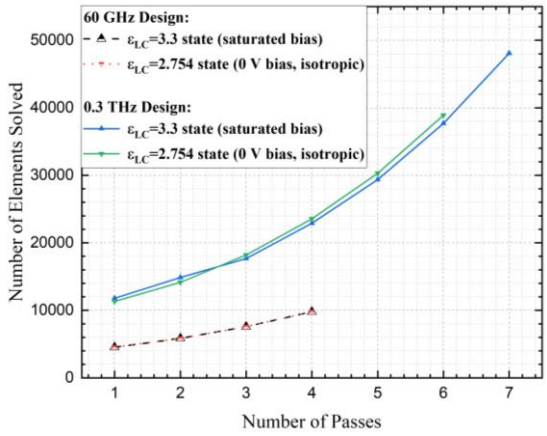

Fig. 4. Number of elements solved for each design and tuning state.

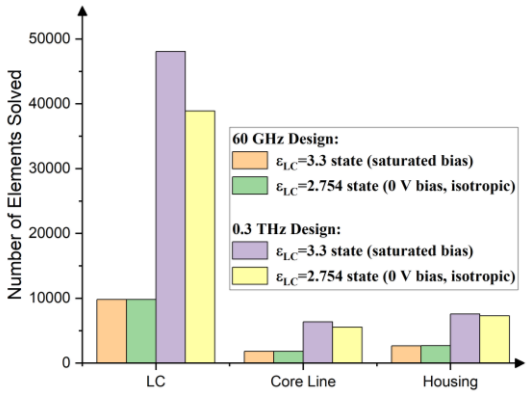

Fig. 5. Number of meshed elements generated in constitutive materials (dielectrics and metals, respectively) for each design and tuning state.

Table 1. Computational Resources Consumed for LC-coaxially-filled Phase Shifter Designs at Diverse Broadband Solution Frequencies (60 GHz design solved from 54 GHz to 66 GHz, 0.3 THz design solved from 225 GHz to 375 GHz, interpolated sweep) and Diverse Tuning States.

Designs and states	Average memory/process	Maximum memory/process	Elapsed time
60 GHz design at ε_{LC}=3.3 state	352 MB	354 MB	00:02:24
60 GHz design at ε_{LC}=2.754 state	355 MB	357 MB	00:02:39
0.3 THz design at ε_{LC} =3.3 state	1.43 GB	1.55 GB	00:06:39
0.3 THz design at ε_{LC} =2.754 state	1.23 GB	1.23 GB	00:05:34

As observed from Fig. 5 and confirmed by Table 1, the 0.3 THz design is far more memory-hungry per process than the 60 GHz mmW design, as evidenced by the 1.43 GB averaged memory per process required at 0.3 THz versus the 352 MB at 60 GHz for the saturated bias state (ε_{LC}=3.3), and the 1.23 GB (0.3 THz design) versus the 355 MB (60 GHz design) for the 0 V bias (LC at isotropic) state. For the 0.3 THz design, from the number of elements (Fig. 5) as well as the averaged memory required per process for the 0.3 THz design, solving the saturated bias state (ε_{LC}=3.3) exhibits a higher number of meshing grids and hence a larger averaged memory required (1.43 GHz on average per process) than that of the isotropic state (ε_{LC} =2.754). From the variable dielectric tuning perspective, this indicates that for the 0.3 THz design, denser field variations (i.e., higher gradients) occur in a higher permittivity medium (than those at a relatively lower permittivity medium). However, such deviation effects that noticeably happen at 0.3 THz are far less pronounced at the 60 GHz design.

Based on the meshing statistics evaluated and documented above, the solutions of the key performance (maximally differential phase shift and worst-case forward transmission coefficient) for the two designs (both in the length of 1 cm, operated at 60 GHz and 0.3 THz, respectively) are obtained and summarised in Fig. 6, from which the corresponding figure-of-merit of each design can be derived by taking the ratio of the maximum phase shift to the maximum insertion loss, as a comprehensive performance indicator for cross-design comparison and benchmark purpose. Interested readers can refer to our recent works [2,3] on the performance optimization of the LC-filled coaxial phase shifters (out of the scope in the current letter that focuses on meshing statistics).

In summary, the memory-hungry and anisotropic dielectric effects that are less computationally sensitive in the 60 GHz millimeter wavelength range for the LC-filled coaxial phase shifter, become prevalent on the THz photonics regime. More specifically at 0.3 THz, the saturated biased state of LC (with the highest achievable permittivity among all tuning states) is most vulnerable to the memory-intensive (time-consuming) problems and hence dominates the computational budget. On the other hand, the highest permittivity state (saturated biasing of LC) indicates the minimally effective wavelength of the modulated wave propagation, which tends to mitigate the low-frequency breakdown (LFB) vulnerability of modern full-wave simulators as raised by [7,8]. The 0 V biased state (isotropic LC) with the lowest permittivity, however, is most susceptible to the LFB risk. Arguably, the meshing implications obtained in this paper can be generalized to influence the development of other LC-based devices or components in the mmW and THz ranges, targeting a selection of deployable applications (e.g., filters, absorbers, impedance adapters) beyond next-generation communications (e.g., remote sensing, security screening).

This study is supported in part by the National Natural Science Foundation of China (NSFC Grant 62301043).

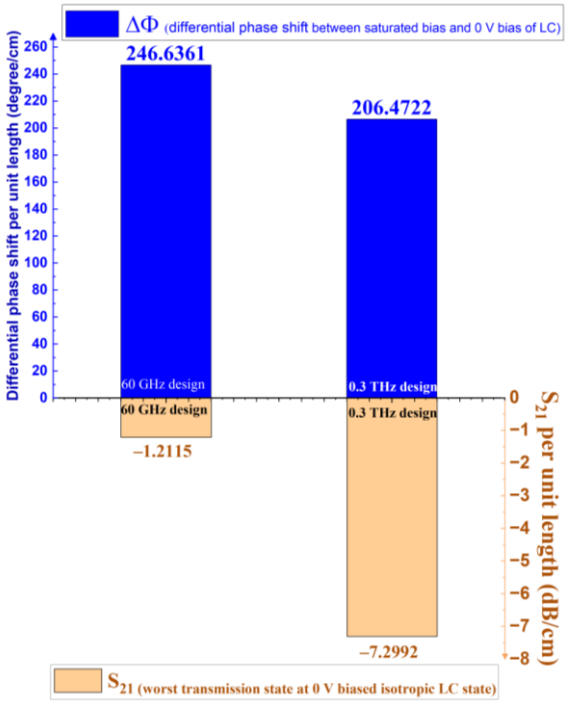

Fig. 6. Computational solutions of differential phase shift and forward transmission coefficient (insertion loss) for the phase shifter designs (60 GHz and 0.3 THz, respectively) based on meshing statistics in this work.

References

[1] M. Makowski, I. Ducin, K. Kakarenko, J. Suszek, A. Kowalczyk, Phot. Lett. Poland **8**, 1 (2016).
[2] J.F. Li, H.R. Li, Electronics **13**, 3 (2024).
[3] J.F. Li, H.R. Li, Crystals **14**, 4 (2024).
[4] J.F. Li, D.P. Chu, Crystals **9**, 12 (2019).
[5] Z. Cendes, *USNC-URSI Radio Science Meeting* (Fajardo, IEEE 2016).
[6] T. Vaupel, *EuCAP* (Copenhagen, IEEE 2020).
[7] L.J. Jiang, W.C. Chew, Microwave Opt. Tech. Lett. **40**, 2 (2004).
[8] J. Zhu, D. Jiao, IEEE Trans. Microw. Theory Tech. **58**, 10 (2010).

